Available on at: www.sciencedirect.com

ScienceDirect

Mitochondrion-targeted PENTATRICOPEPTIDE REPEAT5 is required for *cis*-splicing of *nad4* intron 3 and endosperm development in rice

Long Zhang [a,1,2], *Yanzhou Qi* [a,2], *Mingming Wu* [b,2], *Lei Zhao* [a], *Zhichao Zhao* [a], *Cailin Lei* [a], *Yuanyuan Hao* [b], *Xiaowen Yu* [b], *Yinglun Sun* [b], *Xin Zhang* [a], *Xiuping Guo* [a], *Yulong Ren* [a,*], *Jianmin Wan* [a,b,*]

[a] *National Key Facility for Crop Gene Resources and Genetic Improvement, Institute of Crop Sciences, Chinese Academy of Agricultural Sciences, Beijing 100081, China*

[b] *State Key Laboratory for Crop Genetics and Germplasm Enhancement, Jiangsu Plant Gene Engineering Research Center, Nanjing Agricultural University, Nanjing 210095, Jiangsu, China*

ARTICLE INFO

Article history:
Received 1 July 2020
Received in revised form
29 July 2020
Accepted 7 September 2020
Available online 14 October 2020

Keywords:
Floury endosperm
PPR
Mitochondria
RNA splicing
Oryza sativa

ABSTRACT

Endosperm as the storage organ of starch and protein in cereal crops largely determines grain yield and quality. Despite the fact that several pentatricopeptide repeat (PPR) proteins required for endosperm development have been identified in rice, the molecular mechanisms of many P-type PPR proteins in endosperm development remains unclear. Here, we isolated a rice floury endosperm mutant *ppr5* that developed small starch grains and an abnormal aleurone layer, accompanied by decreased starch, protein, and amylose contents. Map-based cloning combined with a complementation test demonstrated that *PPR5* encodes a P-type PPR protein that is localized to the mitochondria. The mutation in *PPR5* caused reduced splicing efficiency of mitochondrial *NADH dehydrogenase 4* (*nad4*) gene intron 3 and reduced complex I assembly and activity. Loss of *PPR5* function greatly up-regulated expression of alternative oxidases (*AOX*s), reduced ATP production, and affected mitochondrial morphology. We demonstrate that PPR5, as a P-type PPR protein, is required for mitochondrial function and endosperm development by controlling the *cis*-splicing of mitochondrial *nad4* intron 3.

1. Introduction

Rice accumulates large amounts of starch in the endosperm that serves as a carbon source for the plant, human and livestock. Normal endosperm development contributes to grain quality and yield. Rice endosperm has been used as an ideal model system for dissecting the molecular machinery of starch synthesis because of its rich genetic resources and

* Corresponding authors.
E-mail addresses: renyulong@caas.cn (Y. Ren), wanjianmin@caas.cn (J. Wan).
[1] Present Address: College of Bioscience and Biotechnology, Yangzhou University, Yangzhou 225009, Jiangsu, China
[2] These authors contributed equally to this work.

https://doi.org/10.1016/j.cj.2020.09.002

small genome. Many floury endosperm mutants and the causative genes have been identified. Some of them encode enzymes involved in starch synthesis itself, including *ADP-Glucose Pyrophosphorylase Large Subunit 2* (*OsAPL2*), starch synthesis enzyme-encoding gene *OsSSIIIa/FLO5*, and starch branching enzyme-encoding gene *BEIIb/Amylose-extender* (*AE*) [1–3]. Several transcription factors regulate the expression of starch synthesis-related genes, including bHLH144, OsbZIP58, and RSR1 [4–6]. Interestingly, mutations in genes involved in rice storage protein trafficking cause floury endosperm phenotypes, including *GLUTELIN PRECURSOR ACCUMULATION1* (*GPA1*)/*Rab5a*, *GPA2/VPS9a*, *GPA3*, *GPA4/GOT1B*, and *GPA5* [7–11]. Together, these studies suggest that endosperm development involved many biological processes. Novel factors required for endosperm development remain to be explored.

Pentatricopeptide repeat (PPR) proteins are nuclear-encoded proteins characterized by tandem arrays of a degenerate 31–36 amino acid repeat (PPR motif) [12]. PPR proteins generally contain 2–26 PPR motifs and are classified into two subgroups: the classical P-type PPR members composing only of 35-amino acid motifs, and PLS-type PPR members possessing short (S), canonical, and long (L) motifs [13]. Most PPR proteins are predicted to be localized to mitochondria and/or chloroplasts, and are required for the post-transcriptional processing of RNA. Among them, P-type members participate in RNA *cis*- and *trans*-splicing, RNA stabilization, and translational activation, whereas PLS-type members mostly participate in RNA editing [12–14].

Group II introns commonly exist in mitochondrial genome of eukaryotes and encode reverse transcriptase/maturase with catalytic function, which undergo self-splicing [15]. In higher plants, most of group II introns belong to genes encoding subunits of electron transfer chain complex I and require PPR proteins to perform either *cis*-splicing or *trans*-splicing [16]. So far, several P-type PPR proteins have been demonstrated to be involved in intron splicing of mitochondrial transcripts and seed development, such as ABO5, MTL1, TANG2, OTP439, OTP43, and SLO3 in *Arabidopsis thaliana* [17–21], as well as DEK2, DEK35, DEK37, EMP8, EMP10, and EMP16 in maize [22–27]. As PPR proteins are a large family in plants, the underlying splicing mechanisms of numerous unidentified P-type PPR proteins remain poorly understood.

The rice genome contains 491 *PPR* genes, of which 246 *PPR* genes accounting for about 50% belong to P-type, and 245 genes belong to PLS-type [28]. Currently, only four PPR proteins have been identified to be involved in rice mitochondrial function and endosperm development. The mutation in PLS-type PPR protein OGR1 causes a defect in RNA editing at seven specific sites on five mitochondrial genes, inlcuding *nad2*, *nad4*, *cox2*, *cox3*, and *ccmC* [29]. P-type PPR proteins, such as OsNPPR1, OsNPPR3, and FLO10, play an important role in the splicing of mitochondrial genes [30–32]. Compared with the marked progress in Arabidopsis and maize, more P-type PPR proteins involved in intron splicing and endosperm development remain to be identified in rice.

In this study, we identified a novel floury endosperm mutant *ppr5*. Map-based cloning and complementation test demonstrated that *PPR5* encodes a new P-type PPR protein that is localized to mitochondria. Loss of *PPR5* function significantly affected the splicing efficiency of *nad4* intron 3, compromising the assembly of mitochondrial complex I and activity of NADH dehydrogenase. Our results suggest that PPR5 is involved in mitochondrial function and endosperm development in rice by affecting the splicing of mitochondrial *nad4* intron 3.

2. Materials and methods

2.1. Plant materials and growth conditions

The *ppr5* mutant was obtained from an ethyl methanesulfonate (EMS)-induced mutant pool of *japonica* rice cultivar Kitaake. As *ppr5*($^{-/-}$) homozygous mutant plants were seedling lethal, the vitreous brown rice kernels ($^{+/+}$ and $^{+/-}$) was planted for reproduction. A plant which produced seeds with both vitreous and floury endosperm was the *ppr5*($^{+/-}$) heterozygous plant. A *ppr5*($^{+/-}$) heterozygous plant was hybridized with an *indica* variety Dular to produce an F_2 population for map-based cloning. To identify developing endosperm with the mutant phenotype, half-grain assays were performed during grain filling. Briefly, the distal (embryoless) half from *ppr5*($^{+/-}$) heterozygous plant was ground into flour for DNA extraction. Primers 5′-CCCAATAGAGGTGTACGGCT-3′ and 5′-TCCTCACACCATCCTTGCTT-3′ were used for amplification and sequencing of mutation site. The remaining half (with embryo) defective in the *PPR5* gene was used for subsequent experiments. All plants were grown in a paddy field of Institute of Crop Sciences, CAAS in Beijing.

2.2. Microscopy

For the cross-section observations, brown rice was transversely broken by two forceps, coated with gold, and examined with a Hitachi S-4800 scanning electron microscope. Semi-thin sections of endosperms at 9 and 15 days after fertilization (DAF) were prepared according to a previously described process [33]. The sections were counter stained with safranin O and iodine solution, and viewed with an Olympus BX53 light microscope. Given the phenotype difference and technical difficulty to prepare resin section, the grains at 9 DAF were further subjected to ultrastructure observation, RNA extraction, and ATP determination. For ultrastructural observations of mitochondria, endosperms (approximately 2 mm in thickness) at 9 DAF were fixed in 2.5% glutaraldehyde for 24 h, dehydrated and embedded in LR White resin. The samples (approximately 80 nm in thickness) were sectioned using a Leica UC7 ultramicrotome. The sections were examined with a Hitachi H-7650 transmission electron microscope.

2.3. Measurement of starch traits, physicochemical properties, and ATP contents in endosperm

Dry brown rice was ground and passed through a 100 μm mesh sieve to obtain flour. Total starch content was measured with a Megazyme Total Starch Assay kit (K-TSTA). Protein content (N × 5.95) was measured using an Elementar Analysensysteme Gmbh Vario EL cube CHN-Nitrogen analyzer (Elementar, Germany). The amylose content was assessed by the

iodine colorimetric method [33]. The fine structure of amylopectin was measured following a fluorophore-assisted capillary electrophoresis (FACE) method [34]. The pasting properties of brown rice flour were measured using a rapid visco analyzer (RVA, 3D, Newport Scientific, Narrabeen, NSW, Australia). Briefly, a 3 g sample was mixed with 30 mL of H_2O, held at 50 °C for 1 min, progressively heated to 95 °C at 12 °C min^{-1}, held at 95 °C for 2.5 min, cooled to 50 °C at 12 °C min^{-1}, and held at 50 °C for 1.4 min. The ATP contents in developing endosperm of WT and *ppr5* mutant at 9 DAF were measured with an ATP assay kit (Beyotime, Jiangsu).

2.4. Map-based cloning of PPR5

F_1 plants from cross *ppr5*($^{+/-}$)/Dular($^{+/+}$) were of two types, either produced only vitreous brown rice kernels ($^{+/+}$) or both vitreous ($^{+/+}$ and $^{+/-}$) and floury ($^{-/-}$) kernels. A population of 852 floury kernels from the latter were germinated and DNA was extracted from the ultimately lethal F_2 seedlings for gene mapping and map-based cloning using 170 genome-wide polymorphic insertion/deletion (InDel) markers. The sequences of new markers for fine mapping are listed in Table S1.

2.5. Vector construction and rice transformation

For genetic complementation, a 4.6-kb genomic fragment containing the entire *PPR5* coding region, a 2120 bp upstream regulatory region, and a 1083 bp downstream regulatory sequence was cloned by PCR and inserted into the binary vector pCAMBIA1305 to generate the transformation cassette *pCAMBIA1305-PPR5*. The *PPR5* CDS sequence of WT without the stop codon was cloned in-frame in front of the green fluorescent protein (GFP) in the pCAMBIA1305-GFP vector under the control of the *UBIQUITIN1* promoter to create *UBI:PPR5-GFP*. As the *ppr5* floury kernels can induce embryogenic callus, recombinant plasmids *pCAMBIA1305-PPR5* and *UBI:PPR5-GFP* were introduced into *calli* by *Agrobacterium* strain EHA105. Twenty-five independent transgenic lines carrying *pCAMBIA1305-PPR5* and 36 transgenic lines carrying *UBI:PPR5-GFP* were obtained.

2.6. Subcellular localization of PPR5

Wild-type $PPR5^{1-150}$ CDS sequences were amplified and inserted into the pCAMBIA1305-GFP vector under the control of the CaMV 35S promoter to produce a $35S{:}PPR5^{1-150}$-*GFP* plasmid. For transient expression, the plasmid was transfected into *N. benthamiana* leaf epidermal cells as described previously [33]. After 2 days, the *N. benthamiana* leaves were injected with the mitochondrial dye Mitotracker Red (Invitrogen) for 30 mins before imaging. Fluorescent signals were observed using a Zeiss LSM710 confocal laser microscope. *UBI:PPR5-GFP* was transformed into *ppr5* mutant and the roots of T_1 transgenic lines were analyzed using a Zeiss LSM710 confocal laser microscope.

2.7. qRT-PCR and RT-PCR analyses

Total RNA for *PPR5* expression pattern analysis was extracted from WT roots, stems, leaf sheaths, leaves, panicles, and the developing seeds at 3–21 DAF using an RNA Prep Pure Plant kit (Tiangen Co., Beijing, China). First-strand cDNA was reverse transcribed by priming with oligo (dT18) based on a HiScript 1st Strand cDNA Synthesis kit (Vazyme, Nanjing, China). For mitochondrial and *AOX* gene expression analyses, total RNA was extracted from 9 DAF endosperms of WT and *ppr5* mutant, and reverse transcribed using random hexamer primers. Specific primers for RNA splicing analysis were designed for intron–exon (unspliced forms) and exon-exon (spliced forms) links for each gene. Quantitative RT-PCR was performed on a CFX Connect real-time PCR system (Bio-Rad, California, USA) using an AceQ qPCR SYBR Green Master Mix Kit (Vazyme). RT-PCR cycles were adjusted between 24 and 35 depending on the transcript level of the corresponding gene. The rice *Actin* gene was used as an endogenous control. The RT-PCR primers used to analyze 33 mitochondrial genes expression have been documented elsewhere [31], and all the other primers are listed in Table S1.

2.8. Isolation of mitochondria and blue native PAGE

Mitochondria were isolated from endosperm at 9 DAF using the method of Wu [31]. Briefly, approximately 1 g of endosperm was ground in 5 mL of extraction buffer consisting of 75 mmol L^{-1} MOPS-KOH pH 7.6, 0.6 mol L^{-1} sucrose, 4 mmol L^{-1} EDTA, 0.2% polyvinylpyrrolidone 40, 8 mmol L^{-1} Cys, and 0.2% bovine serum albumin. The homogenate was filtered with a two-layer miracloth and centrifuged in a gradient (600, 1300, and 2100×*g* at 4 °C, 4 min each) to remove fiber and debris. The supernatant was centrifuged at 22,000×*g* for 20 min, and resuspended in 400 μL of buffer consisting of 10 mmol L^{-1} MOPS-KOH pH 7.2, 0.3 mol L^{-1} sucrose. After adding 800 μL of distilled water, the suspension was centrifuged again at 22,000×*g* for 20 min to obtain the mitochondria enriched pellet. The pellet was further resuspended in membrane protein extraction buffer consisting of 50 mmol L^{-1} imidazde-HCl pH 7.0, 500 mmol L^{-1} 6-aminohexanoic acid, 1 mmol L^{-1} EDTA, and 1% Triton X-100, incubated on ice for 30 min and centrifuged at 22,000×*g*, 4 °C for 10 min. The supernatant was collected and added to Coomassie Blue G-250 buffer consisting of 5% Coomassie blue G-250, 20 mmol L^{-1} imidazde-HCl pH 7.0, and 500 mmol L^{-1} 6-aminohexanoic acid. 20 μL of mitochondrial protein were loaded onto a 3% to 12% gradient gel to analyze NADH complex I activity in detection buffer (0.02 mol L^{-1} NADH, 1 mmol L^{-1} NBT, and 0.05 mol L^{-1} MOPS-KOH pH 7.6) and stain by Coomassie Blue R-250.

2.9. Circular RT-PCR

Total RNA from endosperm at 9 DAF was extracted and circularized with T4 RNA Ligase (New England Biolabs, Ipswich, MA) following the user's manual. The products were extracted by phenol/chloroform to synthesize the first-strand cDNA by HiScript 1st Strand cDNA Synthesis kit (Vazyme) with specific primer *nad4* exon1-3-cRT (Table S1). The fragments from circular RT-PCR were amplified with specific primers *nad4* exon1-3-cF and *nad4* exon1-3-cR (Table S1), and cloned into the *pEASY*-Blunt Simple Cloning Vector (TransGen, Beijing) for sequencing.

2.10. *Protein extraction and western blot analysis*

Proteins from developing endosperms at 9 DAF were extracted in extraction buffer consisting of 50 mmol L^{-1} Tris-HCl, pH 8.0, 0.25 mol L^{-1} sucrose, 2 mmol L^{-1} DTT, 2 mmol L^{-1} EDTA, 1 mmol L^{-1} phenylmethylsulphonyl fluoride, and protease inhibitor cocktail (Roche). Proteins were transferred to PVDF membranes (0.45 μm, Millipore) after SDS-PAGE. The membranes were incubated with antibodies against AOX and with monoclonal antibody against EF-1α and visualized using a chemiluminescence analyzer (ChemiDocTMX-RS, BioRad).

3. Results

3.1. *Phenotypic characterization of the ppr5 mutant*

The *ppr5* mutant was identified in an ethyl methane sulfonate (EMS)-treated mutant pool of *japonica* rice cultivar Kitaake. Mature grains of *ppr5* with hulls were phenotypically similar to those of WT (Fig. 1A), but the dehulled brown rice of *ppr5* displayed floury endosperm (Fig. 1B). Cross sections of the brown rice kernels showed that the endosperm of *ppr5* was floury-white and shrunken (Fig. 1C, D). Scanning electron microscopy (SEM) indicated that the compound starch grains in endosperm cells of *ppr5* were loosely packed, spherical, and small, in contrast to the densely packed, irregular polyhedral starch grains in WT (Fig. 1E, F). Grain length, width, and thickness of *ppr5* brown rice were significantly reduced (Fig. 1G–I). Correspondingly, the 1000-brown rice grain weight of *ppr5* (11.06 g) was only 51% of WT (21.68 g) (Fig. 1J). Starch, protein, and amylose contents were significantly lower than those in the WT (Fig. 2A-C). Amylopectin fine structure analysis showed proportionate degrees of polymerization (DP) in the range 6–8 and 16–55 were increased in *ppr5*, whereas the proportion in the range 9–15 was significantly decreased relative to the WT (Fig. 2D). Pasting properties of WT and *ppr5* flours determined by a RVA are presented in Fig. 2E, and the pasting parameters are given in Table S2. *ppr5* flour had significantly lower peak viscosity, hot viscosity, breakdown viscosity, and final viscosity than the WT. Moreover, homozygous *ppr5* seedlings showed retarded growth and failed to develop into adult plants (Fig. S1). Thus, the homozygous *ppr5* mutant was defective in endosperm development and vegetative growth, but heterozygous plants with normal growth characteristics produced both normal vitreous and floury brown rice kernels (Fig. S2).

3.2. *The abnormal morphology of compound starch grains and aleurone cells in ppr5 endosperm*

Semi-thin sections of developing endosperms of WT and *ppr5* at 9 and 15 DAF were prepared to observe the starch grain morphologies. Iodine staining showed that the WT produced compound starch grains in endosperm cells (Fig. 3A, a1, C, c1), whereas cells in *ppr5* contained numerous small and single starch grains (Fig. 3B, b1, D, d1). These observations suggested that the *ppr5* mutation affected the formation of normal compound starch grains in the endosperm.

The aleurone cell and ovular vascular trace are considered to function in nutrient transport into the endosperm [31,33]. Saffron O staining showed that the WT had two layers darkly stained aleurone cells, whereas the aleurone cells in *ppr5* were lightly stained and formed more layers than the WT at 9 DAF (Fig. 3A, B), although this was not so evident as that at 15 DAF. However, the cell contents appeared to remain sparse (Fig. 3C, D). As shown in Fig. S3, the ovular vascular traces were largely comparable between developing endosperms in WT and *ppr5* at 9 DAF, but the aleurone cells near the nucellar projection were lightly stained. These results indicated that the *ppr5* mutation obstructed the transport of nutrients into the grain, most likely due to the disrupted development of the aleurone layer.

3.3. *Map-based cloning of PPR5*

A map-based cloning strategy was used to isolate the candidate gene responsible for the *ppr5* mutant phenotype. An F_2 mapping population was created by crossing $ppr5^{(+/-)}$ individuals with the *indica* rice cultivar Dular. A total of 852 floury kernels were selected and germinated, and DNA was extracted from the seedlings for gene mapping. The *PPR5* locus was first mapped between InDel markers ZL5-3 and ZL5-7 on the short arm of chromosome 5. Subsequently, the locus was delimited to an 85-kb region between the InDel markers Z5-14 and Z5-18 on BAC clone OJ1430B02 that contained 10 open reading frames (ORFs) (http://rice.plantbiology.msu.edu/; Fig. 4A). Sequencing analysis of all ORFs revealed a single base (G) deletion in the ORF6 (*Os05g0207200*) at position 421 bp starting from the ATG start codon (Fig. 4B, C; Fig. S4). This mutation formed a new premature stop codon which resulted in a truncated ppr5 protein composed of the N-terminal 160 amino acid residues of WT PPR5 protein (Fig. S5).

To confirm that the single base deletion in *Os05g0207200* was responsible for the mutant phenotype, a 4.6-kb genomic fragment containing the transcriptional regulation elements and the full-length coding sequence of *PPR5* was introduced into the *ppr5* mutant. Positive transgenic lines were selected with recombined vector-specific primers (Fig. 4D). Both brown rice morphology and starch grain phenotype were recovered to WT levels (Fig. 4E, F). These results confirmed that *Os05g0207200* indeed represents *PPR5*.

3.4. *PPR5 encodes a P-type PPR protein*

Sequence analysis showed that *PPR5* comprised a single exon and encoded a protein with 467 amino acid residues (Fig. 5A). Database searches using Pfam [35] revealed that the PPR5 protein contained 7 PPR motifs with a variable degree of conservation and belonged to the P subfamily (Fig. 5A, B). The single base deletion in the *ppr5* allele resulted in loss of all PPR motifs (Fig. 5A). BLAST searches in NCBI showed that *PPR5* is a single-copy gene in the rice genome and its homologous genes widely exist in green algae, bryophytes, pteridophytes, and higher plants (Fig. S6). In summary, PPR5 represents a new member of the P-type PPR protein family in rice.

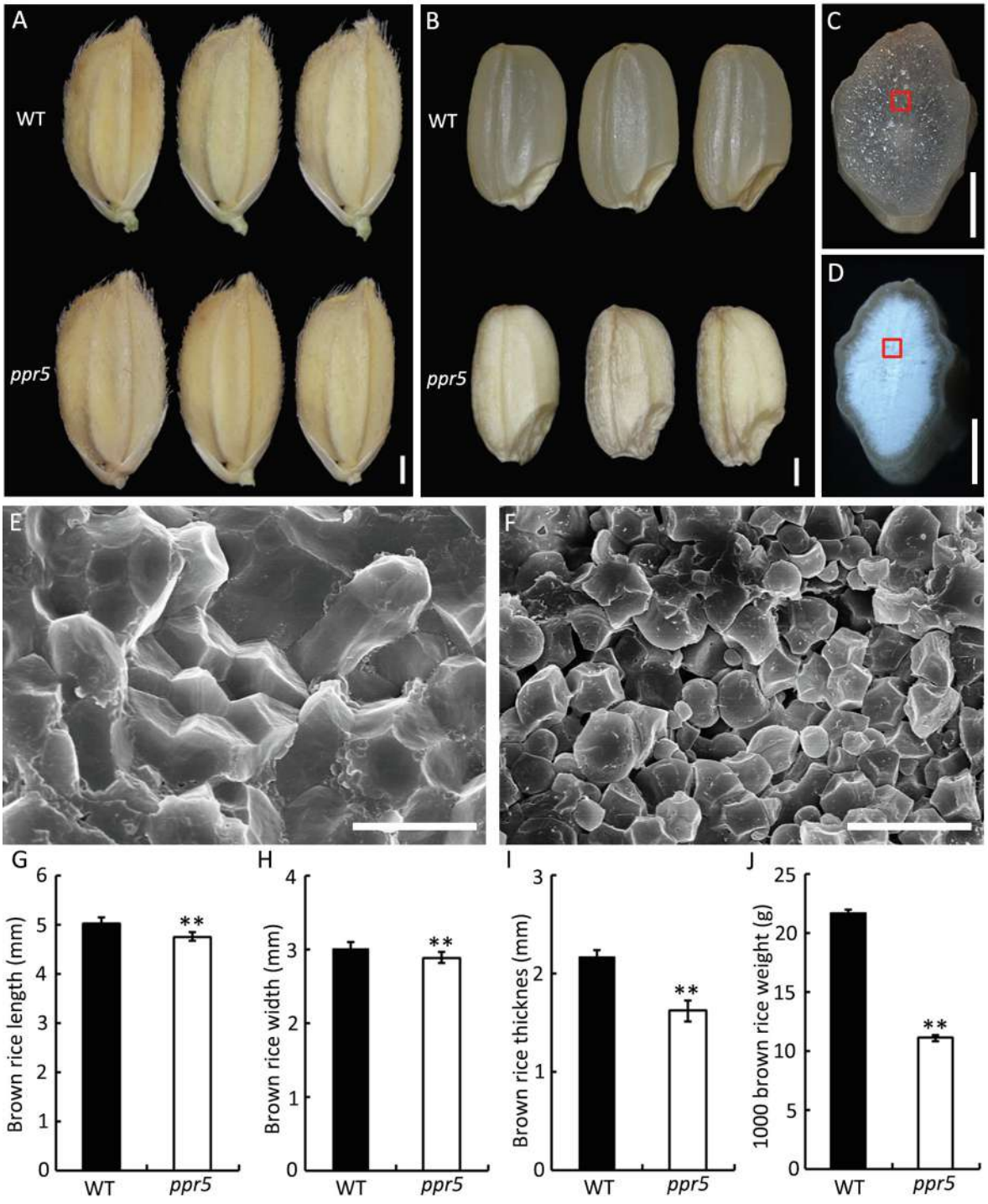

Fig. 1 – Phenotypic analysis of the *ppr5* mutant. (A, B) Morphologies of hulled (A) and brown (B) rice grain of wild type (WT) and *ppr5*. Scale bars, 1 mm. (C, D) Transverse sections of WT (C) and *ppr5* (D) brown rice. Scale bars, 1 mm. (E, F) Scanning electron microscope images of transverse section of WT (E) and *ppr5* (F) brown rice. Scale bars, 10 μm. (G–I) Quantification of brown rice length (G), width (H), and thickness (I) of WT and *ppr5* (n = 30). (J) 1000-brown rice kernel weight of WT and *ppr5* (n = 3). Data are means ± SD from three biological replicates (Student's t-test, **, $P < 0.01$).

3.5. *Expression pattern of PPR5 and subcellular localization of PPR5*

Quantitative RT-PCR assay was performed using tissues from several organs to determine the expression pattern of *PPR5*. Transcripts of *PPR5* were detected in roots, stems, leaves, leaf sheaths, young panicles, and developing endosperm. The highest and the lowest levels of expression were in the leaves and leaf sheaths, respectively (Fig. 5C). In addition, *PPR5* maintained a high expression at the early and middle devel-

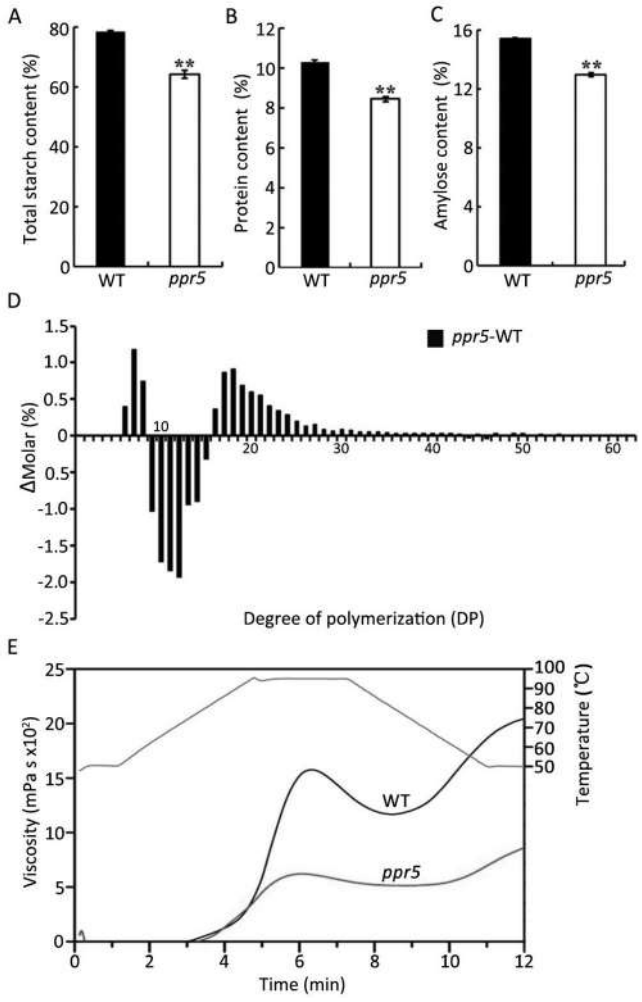

Fig. 2 – Properties of brown rice and amylopectin chain length distribution of flour in *ppr5* compared with WT. (A) Starch, (B) Protein, and (C) Amylose contents; (D) Amylopectin chain length distributions; (E) Rapid viscosity profiles of flours. Data are shown as means ± SD (Student's t-tests, **, $P < 0.01$).

opmental stages in endosperm, and then gradually decreased (Fig. 5C). Consistent with the general expression pattern, *PPR5* plays an important role in seedling growth and endosperm development.

PPR proteins are mainly targeted to chloroplasts or mitochondria, and occasionally to the nucleus [12,30]. To determine the subcellular localization of PPR5, a fusion vector of PPR5 fused with GFP was constructed and transiently expressed in *Nicotiana benthamiana* leaves. Free GFP fluorescence was distributed evenly in the cytoplasm and nuclei, whereas $PPR5^{1-150}$-GFP fluorescence was detected in small dots and co-localized with the red signals from the mitochondrial dye Mitotracker Red (Fig. 5D). To verify the subcellular localization of PPR5 *in vivo*, a fusion vector of full-length PPR5 fused with GFP under the control of the maize *UBIQUITIN1* promoter was constructed and introduced into the *ppr5* mutant. The brown rice grain morphology in the transgenic rice line was well recovered (Fig. S7A), indicating that PPR5-GFP was biologically functional *in vivo*. PPR5-GFP in transgenic root tip cells showed a similar localization pattern (small dots) to that observed in the *N. benthamiana* leaves (Fig. S7B). These data indicated that PPR5 is a mitochondria-localized protein.

3.6. Loss of PPR5 function affects splicing of mitochondrial *nad4* intron 3

The rice mitochondrial genome contains 56 genes, including 34 genes encoding 33 known electron transport chain proteins. Previous studies showed that P-type PPR proteins are involved in mitochondrial RNA metabolism, including cleavage, splicing, stabilization, and translational activation [12,14]. The above amino acid sequence analysis and subcellular localization experiments showed that PPR5 is a mitochondrion-targeted P-type PPR protein. Therefore, transcripts of 33 genes (9 mitochondrial intron-containing genes and 24 other protein-coding genes) in developing endosperms from the WT and *ppr5* at 9 DAF were amplified by RT-PCR using specific primers (Fig. 6A, B). Among 33 genes, only the mature *nad4* transcript was almost undetectable in *ppr5* (Fig. 6A, B). These results indicated that PPR5 was involved in regulation of *nad4* expression in developing endosperm.

Rice mitochondria have 23 group II introns, including 3 introns in the *nad4* sequence. We designed 23 specific primers across adjacent exons to examine the splicing efficiencies of all 23 mitochondrial group II introns in *ppr5* using qRT-PCR. The results showed a significant decrease in splicing efficiency of *nad4* intron 3 in *ppr5* (Fig. 6C). There were also slight reductions in splicing efficiency of *nad4* introns 1 and 2 (Fig. 6C). These results suggested that splicing efficiency of *nad4* intron 3 was reduced in the *ppr5* mutant.

Transcription of mature *nad4* mRNA in rice involves three *cis*-splicing intron events [36]. To verify that the marked reduction in *nad4* in *ppr5* was caused by improper *cis*-splicing of *nad4* intron 3, three specific primers across adjacent exons were designed to examine the *nad4* precursor transcript. RT-PCR analysis showed that introns 1 and 2 were correctly spliced, whereas the *cis*-spliced transcript for exons 3–4 (exon 3 + exon 4) were only weakly detected in *ppr5*, although the precursor of intron 3 was detected (Fig. 7A). Similarly, circular RT-PCR showed that *ppr5* accumulated increased levels of unassembled precursor and decreased levels of mature *nad4* (Fig. 7B). Further sequencing analyses of the amplified products revealed that the end of WT *nad4* mature RNA was similar to that of intron 3 precursor in *ppr5* (Fig. 7C, Fig. S8), indicating that the mutation of *PPR5* does not affect the stability of this precursor. These results suggested that PPR5 is required for the *cis*-splicing of mitochondrial *nad4* intron 3 and formation of the mature *nad4* transcript.

3.7. The mutation in PPR5 affects mitochondrial complex I activity and mitochondrial morphology, and elevates alternative respiratory pathways in mitochondria

nad4 encodes a central subunit of NADH dehydrogenase in mitochondrial complex I. To test whether the *nad4* defect affects the assembly of complex I, we analyzed the mitochon-

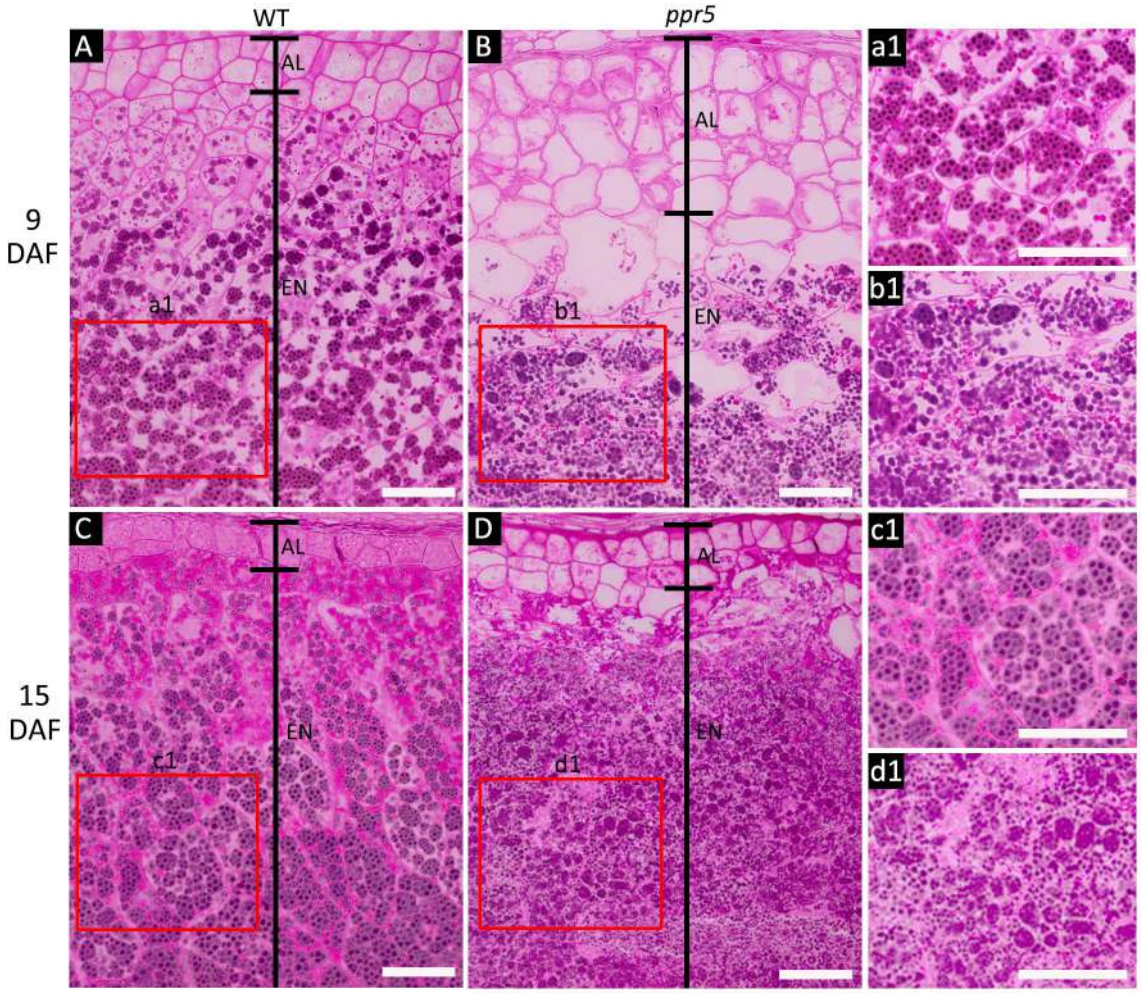

Fig. 3 – Abnormal compound starch grains and aleurone layer in *ppr5* endosperm. (A, B) Safranin O and iodine staining showing the developmental endosperm of WT (A) and *ppr5* (B) at 9 DAF. (a1, b1) represent the magnified regions indicated by red outline in WT and *ppr5* endosperm. (C, D) Safranin O and iodine staining showing the developmental endosperm of WT (C) and *ppr5* (D) at 15 DAF. (c1, d1) represent the magnified regions indicated by red outline in WT (C) and *ppr5* (D) endosperm, respectively. Scale bars, 50 μm. Al, aleurone layer; EN, endosperm.

drial complex by blue native polyacrylamide gel electrophoresis (BN-PAGE). As shown in Fig. 8A, complex I in *ppr5* was significantly reduced compared with the WT. In addition, in-gel NADH-dehydrogenase activity staining analysis showed that the activity of complex I exhibited a dramatic decrease in *ppr5* (Fig. 8B). Since ATP production in mitochondria requires electron transfer through complex I, we measured the ATP content in developing grains at 9 DAF. As shown in Fig. 8C, the ATP content in *ppr5* was about one-third of that in WT. These results suggested that the splicing defect in *nad4* intron 3 caused a functional reduction in the electron transport chain in complex I.

Endosperms from WT and *ppr5* at 9 DAF were observed by transmission electron microscopy (TEM) to detect effects of the *ppr5* mutation on mitochondrial structure. Mitochondria in WT endosperm displayed distinct inner envelope cristae surrounded by a dense matrix, whereas those in *ppr5* were vague in outline and lacked typical cristae (Fig. 8D). These results suggested that the *PPR5* mutation led to the severely impaired mitochondrial function.

Alternative oxidases (AOXs) can be activated in plants when the electron transport chain is disrupted in the cytochrome *c* pathway [37]. To verify whether the disruption in complex I activated an alternative respiratory pathway in *ppr5*, we examined the expression of *AOX* genes (*AOX1A*, *AOX1B*, and *AOX1C*) at the transcriptional level. qRT-PCR showed that both *AOX1A* and *AOX1C* were markedly up-regulated in *ppr5* compared to the WT; *AOX1B* was slightly up-regulated in *ppr5* (Fig. 8E). Immunoblotting analysis showed that AOX proteins were also dramatically increased in *ppr5* (Fig. 8F). These data strongly suggested that the *PPR5* mutation altered the assembly and activity of complex I, leading to up-regulated expression of genes in the alternative respiratory pathway.

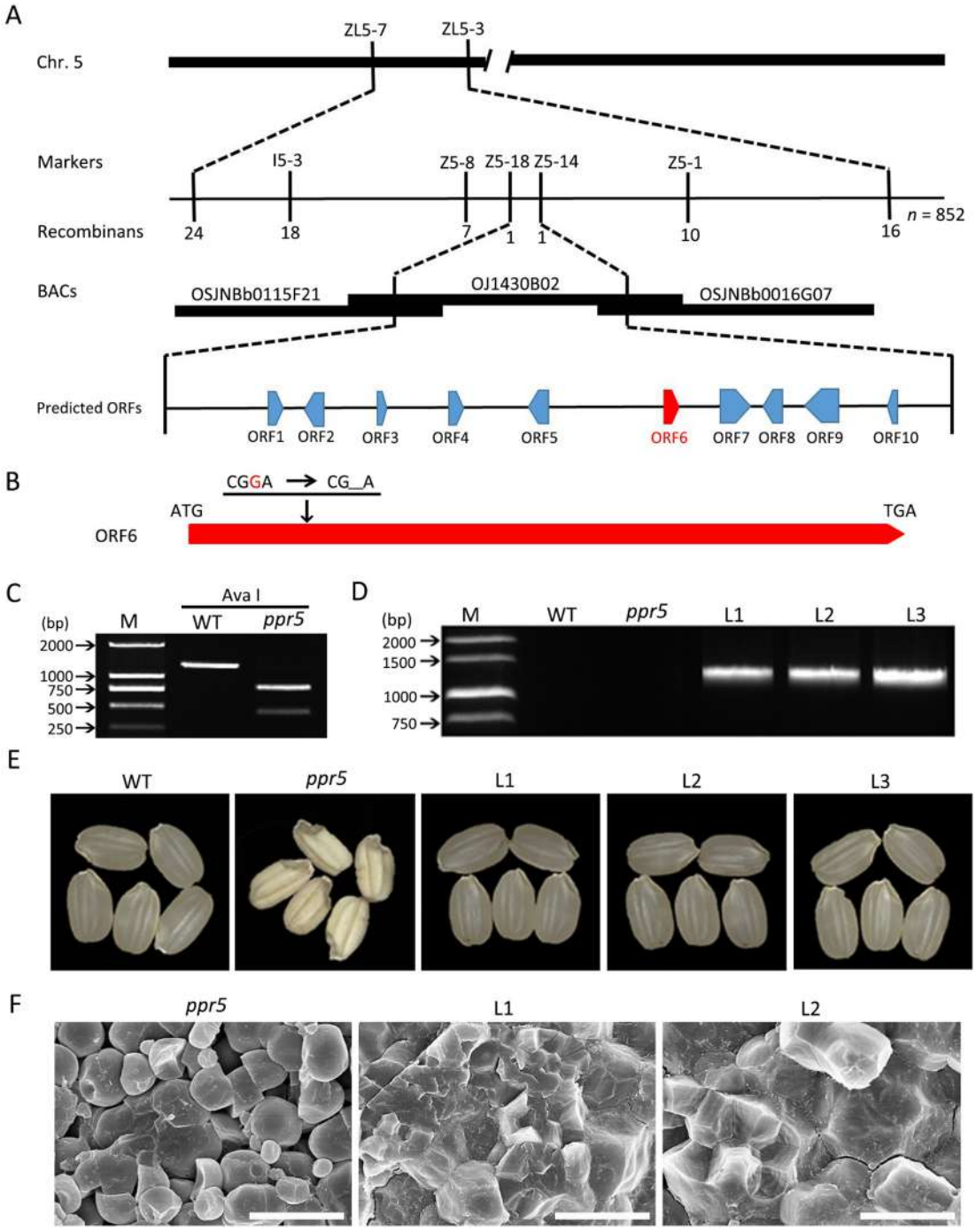

Fig. 4 – Map-based cloning of the PPR5 locus and genetic complementation of the *ppr5* mutant. (A) Fine mapping of the PPR5 locus (red arrow). The locus was mapped to an 85-kb region between markers Z5-14 and Z5-18 on the short arm of chromosome 5 that contains 10 open reading frames (ORFs). (B) A single base (G) was deleted in ORF6 (*Os05g0207200*) at position 421 bp from the ATG start codon. (C) Molecular identification of the single base deletion by a CAPS marker. The left and right panels showed the CAPS analysis associated with WT and *ppr5*. M, marker. (D) Molecular identification of transgenic plants by PCR amplification. M, marker. (E, F) Complementation of the *ppr5* mutation restored to normal brown rice appearance (E) and starch grain morphology (F). Scale bars, 10 μm.

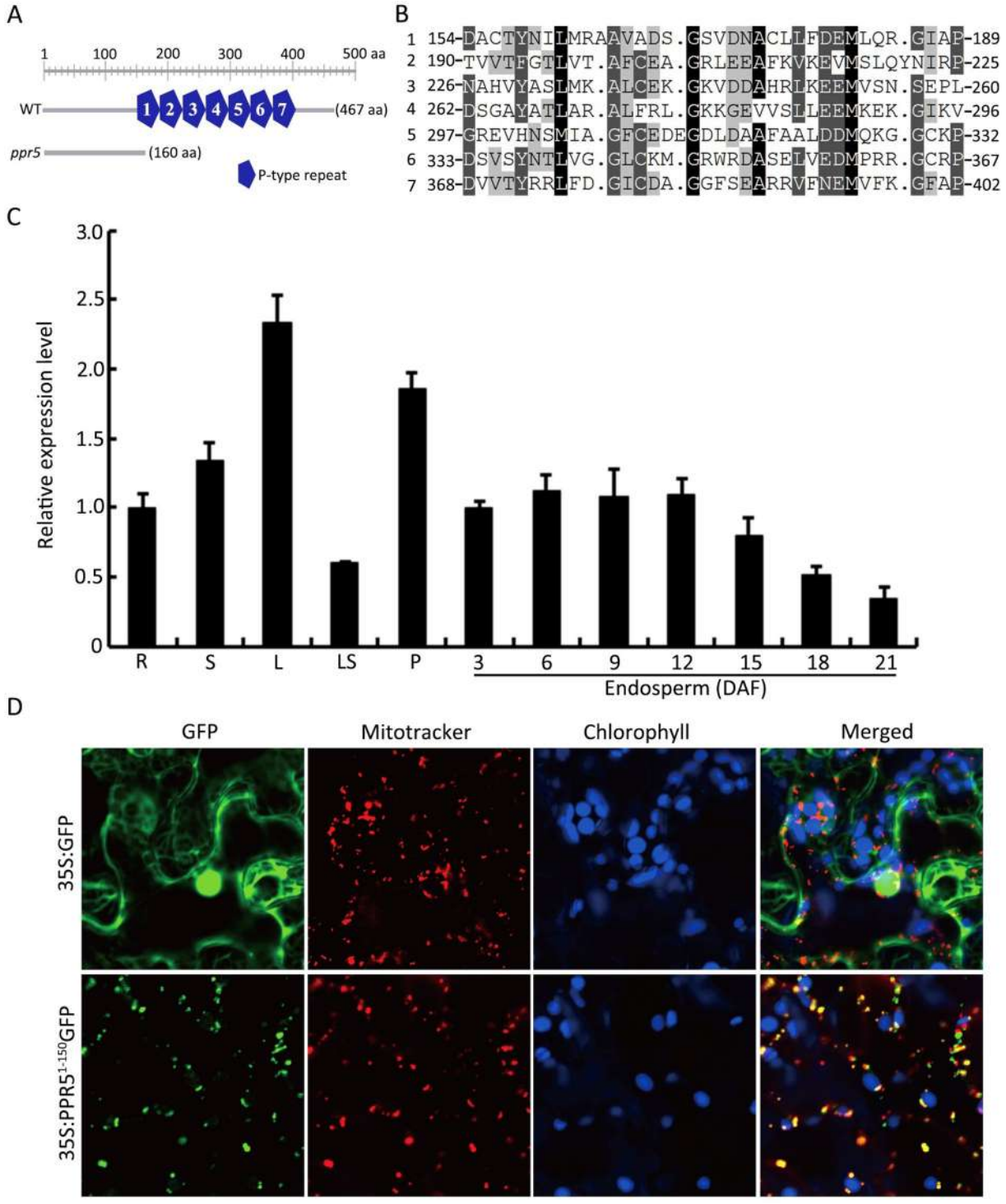

Fig. 5 – Expression pattern of PPR5 and subcellular localization of PPR5. (A) PPR5 protein contained 7 PPR motifs, whereas the mutated ppr5 protein putatively had no PPR motifs. (B) Amino acid sequences of 7 PPR motifs of PPR5. Amino acids fully or semiconserved are shaded black and gray, respectively. (C) Expression pattern of *PPR5* in various rice tissues and in the endosperm at different developmental stages. R, root; S, stem; L, leaf; LS, leaf sheath; P, panicle. (D) Subcellular localization of PPR5 in *N. benthamiana* leaves. Panels display transient expression of free GFP and $PPR5^{1-150}$-GFP (green), Mitotracker localization (red), chlorophyll autofluorescence (blue), and merged images. Scale bars, 10 μm.

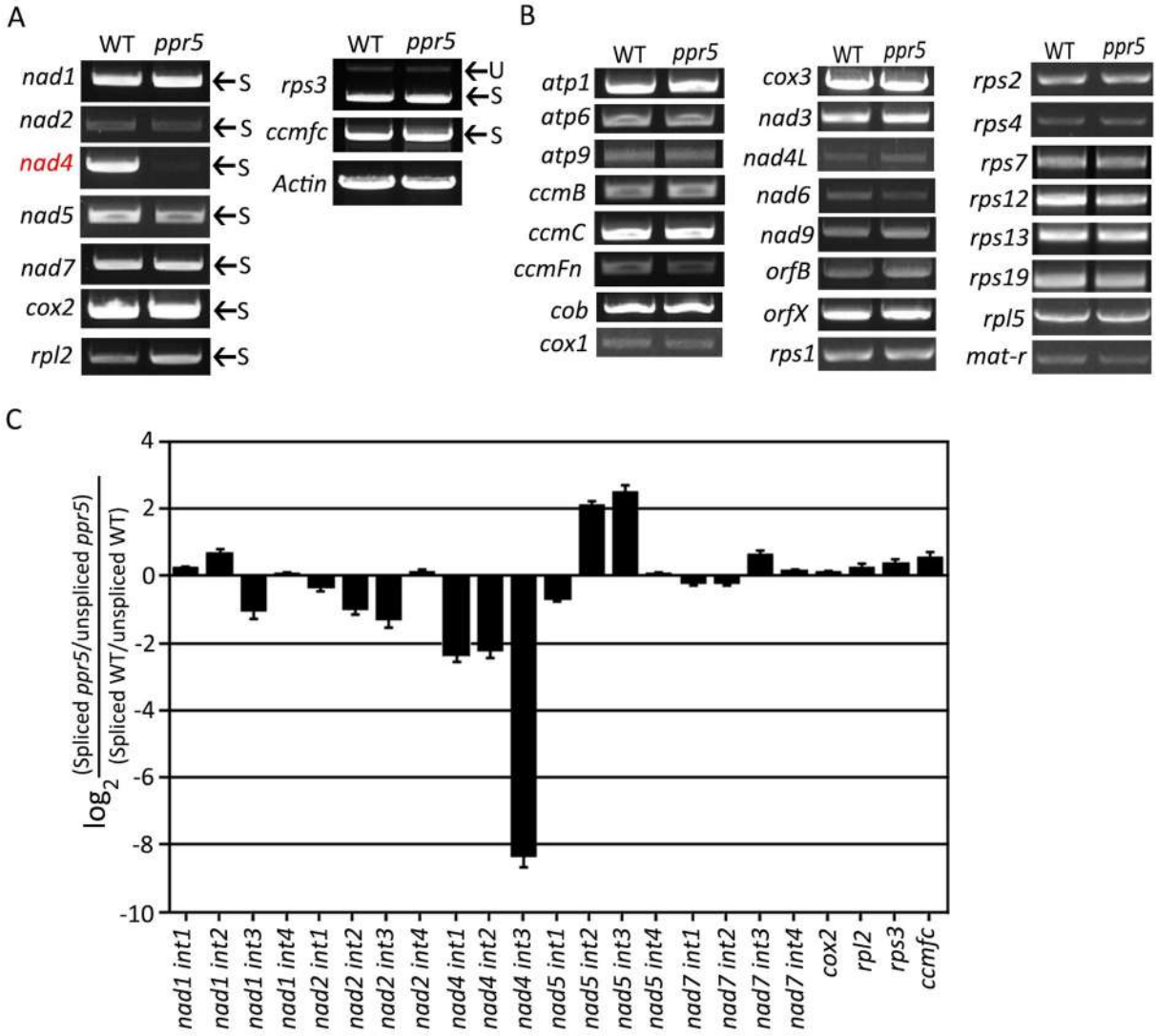

Fig. 6 – Loss of mature *nad4* transcript and splicing deficiency of *nad4* intron 3 in *ppr5* endosperm. (A, B) RT-PCR analyses of expression of 9 intron-containing (A) and other protein-encoding (B) genes in the mitochondrial genome in WT and *ppr5*. *Actin* was used as a sample loading control. U, unspliced; S, spliced. (C) Quantitative RT-PCR analysis of 23 group II introns of mitochondrial genes in WT and *ppr5*. Primers spanning adjacent exons and introns were used to measure differences in splicing efficiency. Data are shown as means ± SD from three biological replicates.

4. Discussion

4.1. The *ppr5* mutation caused defective mitochondrial function and endosperm development

Rice endosperm has been a preferred system to explore regulatory mechanisms of starch and/or protein synthesis [38,39]. Defects in endosperm development generally affect starch and/or protein accumulation leading to loss in grain weight and/or changes in amylose: amylopectin ratio. Previous studies have indicated that the accumulation of starch and protein maintains a balance during endosperm development, when one increases, the other decreases. For example, starch synthesis in *flo6*, *flo8*, *gif2*, and *pdil1-1* mutants is disordered, and starch content decreases while the protein content increases [34,40–42]. In this study, we isolated and identified a rice floury endosperm *ppr5* mutant that exhibited several distinct features. As the starch and protein contents were significantly reduced, the grain weight of *ppr5* was severely reduced compared to WT (Fig. 1J and 2A, B). The amylose content and amylopectin fine structure also differed between WT and *ppr5* (Fig. 2C, D). The endosperm phenotype caused by the *ppr5* mutation is more severe than those of mutants reported previously. This is likely due to the lethality of homozygous mutant plants compared to those mutants such as *flo6*, *flo7*, and *flo8* [33,40,41]. Therefore, a leaky mutation in *PPR5* may lead to a weak phenotypic change, which can be used for grain quality improvement in the future. Despite the fact that most of the defective endosperm mutants exhibit a floury-white appearance, they differ in starch grain morphology. For example, loss-of-function mutation of *SSG5* and *ISA1* seriously inhibits initiation of starch grains and results in

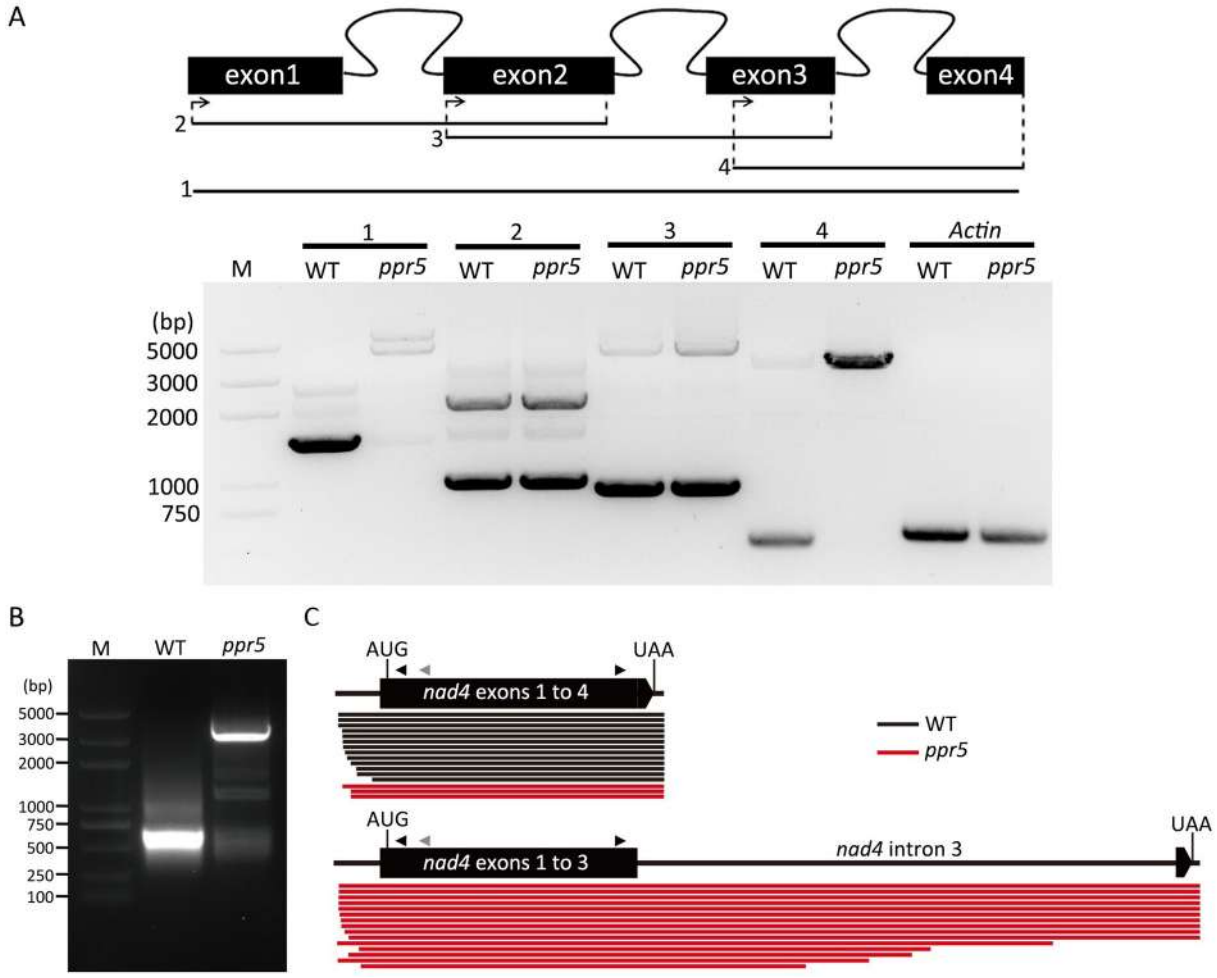

Fig. 7 – *ppr5* accumulates unassembled precursors of *nad4* intron 3. (A) Gene structure of mitochondrial *nad4* and RT-PCR analysis of three *nad4* introns in WT and *ppr5*. Numbers represent primers for different amplification products. M, marker. (B) Agarose gel electrophoretic detection of circular RT-PCR amplification products of *nad4* exons 1–3. p, exons 1–3 precursor; m, mature *nad4*. (C) Mapping of the circular RT-PCR products as determined by sequencing of *nad4* exons 1–3. Each bar represents a single sequenced clone and shows the position of the 5′ and 3′ extremities.

accumulation of phytoglycogen [43,44]; and mutations in *SSG4* and *SSG6* cause enlarged starch grains in the endosperm [45,46]. By contrast, endosperm development in *ppr5* kernels was delayed, leading to the formation of a large number of small and single starch grains (Fig. 3).

Tissues that are responsible for the nutrition transportation in maize endosperm include the basal endosperm transfer layer (BETL) and aleurone. BETL occurs at the endosperm surface near the vascular bundle at the base of the kernel and develops from a layer of cells to a multilayer of cells with grain filling [47]. Previous studies identified several loss-of-function mutations in mitochondrial-localized PPR proteins in maize, including Dek2, Dek35, Dek37, EMP8, and EMP10 [22–26] that affected mitochondrial function and development of BETL, leading to stagnation of endosperm development and lethal seedlings. The phenotype of rice *ppr5* was very similar to those of maize mutants with defective mitochondria-localized PPR proteins, abnormal endosperm development, and seedling lethality (Fig. 1 and Fig. S1). In rice, the aleurone layer and ovular vascular trace, rather than the BETL, are considered to function in transporting nutrients into the endosperm, an energy-dependent process [31]. Compared with starchy endosperm cells which are near oxygen-free and have few mitochondria, aleurone cells have 8% oxygen concentrations and contain abundant mitochondria [48]. Our microscopic observations revealed that the endosperm of *ppr5* showed no significant difference in the ovular vascular trace compared with WT (Fig. S3), but aleurone development was abnormal, most likely related to the dysfunctional mitochondria (Figs. 3 and 8D). Since the ATP content in *ppr5* endosperm was significantly lower than in the WT (Fig. 8C), it was likely that the defective aleurone layer in *ppr5* with abnormal mitochondrial function could not import sufficient nutrients into the developing grain and cause stress, leading to the floury and shrunken endosperm phenotype.

4.2. *PPR5 affects the mitochondrial nad4 intron 3 splicing*

More than 20 group II introns that exist in the mitochondrial genome in flowering plants require either *cis*- or *trans*-splicing

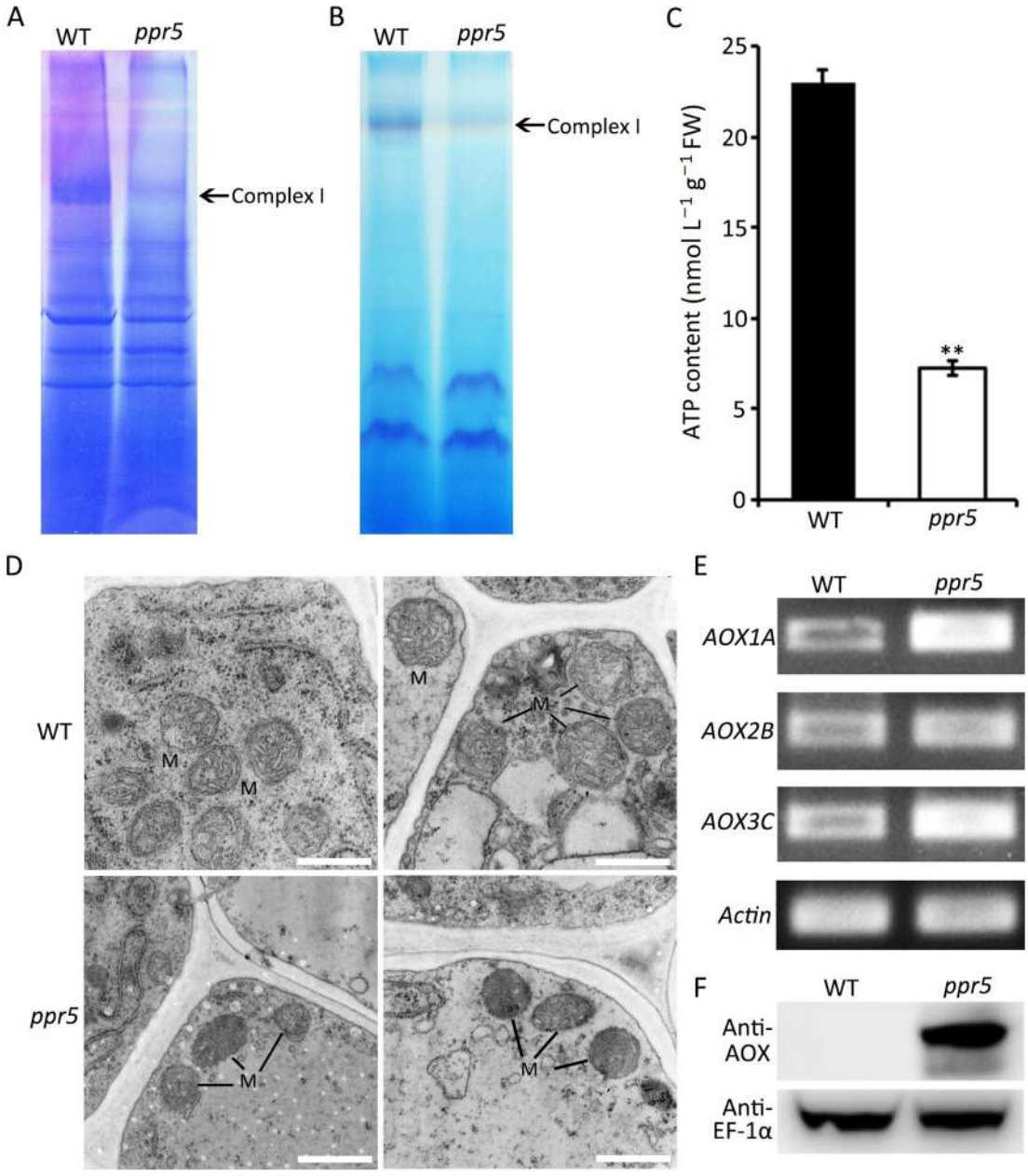

Fig. 8 – Loss of PPR5 function disrupted mitochondrial function. (A) Blue native PAGE analysis of mitochondrial complex I. (B) In-gel NADH-dehydrogenase activity analysis of mitochondrial complex I. (C) ATP concentration in grains at 9 DAF. (D) Transmission electron microscopy of mitochondria in WT and *ppr5* endosperm at 9 DAF. M, mitochondria. (E) RT-PCR analysis of *AOX1A*, *AOX1B*, and *AOX1C* involved in the alternative respiratory pathway. *Actin* was used as a sample loading control. (F) Immunoblotting analysis of AOX proteins in the developing endosperm of WT and *ppr5* kernels. Anti-EF-1α antibodies were used as loading control. Data are shown as means ± SD from three biological replicates, and compared with WT by Student's *t*-test (, $P < 0.01$).**

[36]. P-type PPR proteins involved in group II intron splicing have been extensively studied in Arabidopsis and maize. Here, we identified PPR5 as a regulator required for endosperm development in rice through control of mitochondrial *nad4* intron 3 splicing. Most group II introns belong to genes encoding subunits in complex I (NADH dehydrogenase), including *cis*-spliced introns in *nad1*, *nad2*, *nad4*, *nad5*, and *nad7* as well as *trans*-spliced introns in *nad1*, *nad2*, and *nad5* [36]. MTSF2/PPR19, nMAT1, OTP43, DEK2, and FLO10 were identified as *trans*-splicing factors in *nad1* in Arabidopsis, maize, and rice [18,25,31,49,50]. Dek37 and EMP16 are specifically required for *cis*-splicing of *nad2* intron 1 and intron 4 in maize [24,27]. Dek35 was shown to participate in *cis*-splicing of *nad4* intron 1 [23]. MTL1 is required for both translation and splicing of mitochondrial *nad7* mRNA in Arabidopsis [20]. PPR5 identified in this study is a P-type PPR protein containing 7 predicted PPR motifs. Splicing analyses combined with circular RT-PCR demonstrated that *cis*-splicing of *nad4*

intron 3 was significantly disrupted in *ppr5* (Fig. 7), suggesting that PPR5 is crucial for *nad4* intron 3 splicing in rice mitochondria. Previous studies have shown that P-type PPR proteins can bind to the 5′ or 3′ ends of their substrates to provide a barrier to exoribonucleases or to remodel target RNA [31,51]. Loss-of-function mutations of mitochondrion-targeted PPR protein usually cause reduced stability of targeted transcripts. For example, PPR78 is required for the stability of *nad5*T1 precursor and *nad5* mature mRNA in maize. In the *ppr78* mutant, the abundance of intron 1 and/or 2 spliced transcripts is significantly decreased [52]. No significant difference in the 5′ and 3′ extremities of *nad4* precursor in *ppr5* were detected (Fig. 7C, Fig. S8), but the amounts of unassembled precursors were increased (Fig. 7). Therefore, PPR5 is required for intron splicing, but does not affect the stability of the precursor, which may be inconsistent with the function of PPR78 protein. A deletion of the single base G leading to premature termination of the PPR5 protein caused a loss of all PPR motifs (Fig. 4B and 5A). Hence, the ppr5 protein corresponded to a loss-of-function mutant of *PPR5*, but the mature *nad4* transcript was not completely abolished in *ppr5*. This indicated that splicing of *nad4* intron 3 might also involve other proteins.

4.3. *Post-transcriptional processing of the nad4 transcript is crucial for mitochondrial function*

NADH dehydrogenase is the major entry point for electron transport that involves nine mitochondrially encoded subunits, including NAD1-4, NAD4L, NAD5-7, and NAD9 [23]. Several PPR proteins have been reported to function in the diverse RNA processing of the *nad4* transcript in Arabidopsis, maize, and rice (Table S3). EMP8, Dek35, DEK41/DEK43, and RL1 affect the *cis*-splicing of *nad4* intron 1 and/or 3 [23,26,53–55], AHG11 is involved in *nad4* RNA editing [56], RPF1 is required for 5′-end processing [57], MTSF1 stabilizes the *nad4* mRNA [51]. All these studies suggested that NAD4 plays a vital role in mitochondrial function. Supporting this notion, we identified the rice homolog of maize *DEK41/DEK43* (Fig. S6) and found that its loss-of-function mutation results in a deficiency in mitochondrial complex I assembly and activity, and leading to seedling lethality and abnormal endosperm development (Figs. 3, 7 and 8). Our study demonstrated that correct splicing of the *nad4* transcript is a crucial posttranscriptional step in maintaining normal function of mitochondrial complex I in rice.

CRediT authorship contribution statement

Jianmin Wan supervised the project. Jianmin Wan and Yulong Ren designed the research. Yulong Ren screened the mutant material. Long Zhang, Yanzhou Qi, and Mingming Wu performed experiments. Lei Zhao, Zhichao Zhao, Cailin Lei, Yuanyuan Hao, Yinglun Sun, Xiaowen Yu, Xin Zhang, and Xiuping Guo provided technical assistance. Long Zhang and Yulong Ren analyzed the data and drafted the manuscript. Jianmin Wan improved the manuscript. All authors discussed the results and commented on the manuscript.

Declaration of competing interest

Authors declare that there are no conflicts of interest.

Acknowledgments

This work was supported by grants from the National Natural Science Foundation of China (31901427), the National Transgenic Science and Technology Program (2019ZX08010-003), the Agricultural Science and Technology Innovation Program of CAAS (CAAS-ZDXT2018001) and the Young Talent of CAAS to Yulong Ren.

Appendix A. Supplementary data

Supplementary data this article can be found online at https://doi.org/10.1016/j.cj.2020.09.002.

REFERENCES

[1] Nishi A, Nakamura Y, Tanaka N, Satoh H. Biochemical and genetic analysis of the effects of amylose-extender mutation in rice endosperm. Plant Physiol. 2001;127:459–72.
[2] Ryoo N, Yu C, Park C-S, Baik M-Y, Park IM, Cho M-H, Bhoo SH, An G, Hahn T-R, Jeon J-S. Knockout of a starch synthase gene *OsSSIIIa/Flo5* causes white-core floury endosperm in rice (*Oryza sativa* L.). Plant Cell Rep. 2007;26:1083–95.
[3] Zhang D, Wu J, Zhang Y, Shi C. Phenotypic and candidate gene analysis of a new floury endosperm mutant (*osagpl2-3*) in rice. Plant Mol. Biol. Rep. 2012;30:1303–12.
[4] Bello BK, Hou Y, Zhao J, Jiao G, Wu Y, Li Z, Wang Y, Tong X, Wang W, Yuan W, Wei X, Zhang J. NF-YB1-YC12-bHLH144 complex directly activates *Wx* to regulate grain quality in rice (*Oryza sativa* L.). Plant Biotechnol. J. 2019;17:1222–35.
[5] Fu F-F, Xue H-W. Coexpression analysis identifies rice starch regulator1, a rice AP2/EREBP family transcription factor, as a novel rice starch biosynthesis regulator. Plant Physiol. 2010;154:927–38.
[6] Wang JC, Xu H, Zhu Y, Liu QQ, Cai XL. OsbZIP58, a basic leucine zipper transcription factor, regulates starch biosynthesis in rice endosperm. J. Exp. Bot. 2013;64:3453–66.
[7] Liu F, Ren Y, Wang Y, Peng C, Zhou K, Lv J, Guo X, Zhang X, Zhong M, Zhao S, Jiang L, Wang H, Bao Y, Wan J. OsVPS9A functions cooperatively with OsRAB5A to regulate post-Golgi dense vesicle-mediated storage protein trafficking to the protein storage vacuole in rice endosperm cells. Mol. Plant 2013;6:1918–32.
[8] Ren Y, Wang Y, Liu F, Zhou K, Ding Yu, Zhou F, Wang Y, Liu K, Gan Lu, Ma W, Han X, Zhang X, Guo X, Wu F, Cheng Z, Wang J, Lei C, Lin Q, Jiang L, Wu C, Bao Y, Wang H, Wan J. *GLUTELIN PRECURSOR ACCUMULATION3* encodes a regulator of post-golgi vesicular traffic essential for vacuolar protein sorting in rice endosperm. Plant Cell 2014;26:410–25.
[9] Ren Y, Wang Y, Pan T, Wang Y, Wang Y, Gan Lu, Wei Z, Wang F, Wu M, Jing R, Wang J, Wan G, Bao X, Zhang B, Zhang P, Zhang Yu, Ji Yi, Lei C, Zhang X, Cheng Z, Lin Q, Zhu S, Zhao Z, Wang J, Wu C, Qiu L, Wang H, Wan J. *GPA5* encodes a Rab5a effector required for post-Golgi trafficking of rice storage proteins. Plant Cell 2020;32:758–77.
[10] Wang YH, Ren YL, Liu X, Jiang L, Chen LM, Han XH, Jin MN, Liu SJ, Liu F, Lv J, Zhou KN, Su N, Bao YQ, Wan JM. OsRab5a regulates endomembrane organization and storage protein trafficking in rice endosperm cells. Plant J. 2010;64:812–24.

[11] Wang Y, Liu F, Ren Y, Wang Y, Liu Xi, Long W, Wang Di, Zhu J, Zhu X, Jing R, Wu M, Hao Y, Jiang L, Wang C, Wang H, Bao Y, Wan J. GOLGI TRANSPORT 1B regulates protein export from the endoplasmic reticulum in rice endosperm cells. Plant Cell 2016;28:2850–65.
[12] Lurin C, Andrés C, Aubourg S, Bellaoui M, Bitton F, Bruyère C, Caboche M, Debast C, Gualberto J, Hoffmann B, Lecharny A, Le Ret M, Martin-Magniette M-L, Mireau H, Peeters N, Renou J-P, Szurek B, Taconnat L, Small I. Genome-wide analysis of arabidopsis pentatricopeptide repeat proteins reveals their essential role in organelle biogenesis. Plant Cell 2004;16:2089–103.
[13] Linneweber C, Small I. Pentatricopeptide repeat proteins: a socket set for organelle gene expression. Trends Plant Sci. 2008;13:663–70.
[14] Barkan A, Small I. Pentatricopeptide repeat proteins in plants. Annu. Rev. Plant Biol. 2014;65:415–42.
[15] Michel F, Ferat J. Structures andactivities of group II introns. Annu. Rev. Biochem. 1995;64:435–61.
[16] Berrisford JM, Sazanov LA. Structural basis for the mechanism of respiratory complex I. J. Biol. Chem. 2009;284:29773–83.
[17] Colas des Francs-Small C, Falcon de Longevialle A, Li Y, Lowe E, Tanz SK, Smith C, Bevan MW, Small I. The pentatricopeptide repeat proteins TANG2 and ORGANELLE TRANSCRIPT PROCESSING439 are involved in the splicing of the multipartite *nad5* transcript encoding a subunit of mitochondrial complex I. Plant Physiol. 2014;165:1409–16.
[18] de Longevialle AF, Meyer EH, Andrés C, Taylor NL, Lurin C, Millar AH, Small ID. The pentatricopeptide repeat gene *OTP43* is required for trans-splicing of the mitochondrial *nad1* intron 1 in Arabidopsis thaliana. Plant Cell 2007;19:3256–65.
[19] Hsieh W-Y, Liao J-C, Chang C-Y, Harrison T, Boucher C, Hsieh M-H. The SLOW GROWTH3 pentatricopeptide repeat protein is required for the splicing of mitochondrial NADH dehydrogenase subunit7 intron 2 in Arabidopsis. Plant Physiol. 2015;168:490–501.
[20] Haïli N, Planchard N, Arnal N, Quadrado M, Vrielynck N, Dahan J, Francs-Small CCD, Mireau H. The MTL1 pentatricopeptide repeat protein is required for both translation and splicing of the mitochondrial NADH dehydrogenase subunit7 mRNA in Arabidopsis. Plant Physiol. 2016;170:354–66.
[21] Liu Y, He J, Chen Z, Ren X, Hong X, Gong Z. *ABA overly-sensitive 5 (ABO5)*, encoding a pentatricopeptide repeat protein required for *cis*-splicing of mitochondrial *nad2* intron 3, is involved in the abscisic acid response in Arabidopsis. Plant J. 2010;63:749–65.
[22] Cai M, Li S, Sun F, Sun Q, Zhao H, Ren X, Zhao Y, Tan B-C, Zhang Z, Qiu F. *Emp10* encodes a mitochondrial PPR protein that affects the *cis* -splicing of *nad2* intron 1 and seed development in maize. Plant J. 2017;91:132–44.
[23] Chen X, Feng F, Qi W, Xu L, Yao D, Wang Q, Song R. *Dek35* encodes a PPR protein that affects *cis*-splicing of mitochondrial *nad4* intron 1 and seed development in maize. Mol. Plant 2017;10:427–41.
[24] Dai D, Luan S, Chen X, Wang Q, Feng Y, Zhu C, Qi W, Song R. Maize *Dek37* encodes a P-type PPR protein that affects *cis*-splicing of mitochondrial *nad2* Intron 1 and seed development. Genetics 2018;208:1069–82.
[25] Qi W, Yang Y, Feng X, Zhang M, Song R. Mitochondrial function and maize kernel development requires Dek2, a pentatricopeptide repeat protein involved in *nad1* mRNA splicing. Genetics 2017;205:239–49.
[26] Sun F, Zhang X, Shen Y, Wang H, Liu R, Wang X, Gao D, Yang Y-Z, Liu Y, Tan B-C. The pentatricopeptide repeat protein EMPTY PERICARP8 is required for the splicing of three mitochondrial introns and seed development in maize. Plant J. 2018;95:919–32.
[27] Xiu Z, Sun F, Shen Y, Zhang X, Jiang R, Bonnard G, Zhang J, Tan B-C. EMPTY PERICARP16 is required for mitochondrial *nad2* intron 4 *cis*-splicing, complex I assembly and seed development in maize. Plant J. 2016;85:507–19.
[28] Chen G, Zou Y, Hu J, Ding Y. Genome-wide analysis of the rice PPR gene family and their expression profiles under different stress treatments. BMC Genomics 2018;19:720.
[29] Kim SR, Yang JI, Moon S, Ryu CH, An K, Kim KM, Yim J, An G. Rice OGR1 encodes a pentatricopeptide repeat-DYW protein and is essential for RNA editing in mitochondria. Plant J. 2009;59:738–49.
[30] Hao YY, Wang YL, Wu MM, Zhu XP, Teng X, Sun YL, Zhu JP, Zhang YY, Jing RN, Lei J, Li JF, Bao XH, Wang CM, Wang YH, Wan JM. The nuclear-localized PPR protein OsNPPR1 is important for mitochondrial function and endosperm development in rice. J. Exp. Bot. 2019;70:4705–19.
[31] Wu MM, Ren YL, Cai MH, Wang YL, Zhu SS, Zhu JP, Hao YY, Teng X, Zhu XP, Jing RN, Zhang H, Zhong MS, Wang YF, Lei CL, Zhang X, Guo XP, Cheng ZJ, Lin QB, Wang J, Jiang L, Bao YQ, Wang YH, Wan JM. Rice *FLOURY ENDOSPERM10* encodes a pentatricopeptide repeat protein that is essential for the *trans*-splicing of mitochondrial *nad1* intron 1 and endosperm development. New Phytol. 2019;223:736–50.
[32] Xue MY, Liu LL, Yu YF, Zhu JP, Gao H, Wang YH, Wan JM. Lose-of-function of a rice nucleolus-localized pentatricopeptide repeat protein is responsible for the *floury endosperm14* mutant phenotypes. Rice 2019;12:100.
[33] Zhang L, Ren Y, Lu B, Yang C, Feng Z, Liu Z, Chen J, Ma W, Wang Y, Yu X, Wang Y, Zhang W, Wang Y, Liu S, Wu F, Zhang X, Guo X, Bao Y, Jiang L, Wan J. *FLOURY ENDOSPERM7* encodes a regulator of starch synthesis and amyloplast development essential for peripheral endosperm development in rice. J. Exp. Bot. 2016;67:633–47.
[34] Han XH, Wang YH, Liu X, Jiang L, Ren YL, Liu F, Peng C, Li JJ, Jin XM, Wu FQ, Wang JL, Guo XP, Zhang X, Cheng ZJ, Wan JM. The failure to express a protein disulphide isomerase-like protein results in a floury endosperm and an endoplasmic reticulum stress response in rice. J. Exp. Bot. 2012;63:121–30.
[35] Finn RD, Mistry J, Schuster-Bockler B, Griffiths-Jones S, Hollich V, Lassmann T, Moxon S, Marshall M, Khanna A, Durbin R, Eddy SR, Sonnhammer ELL, Bateman A. Pfam: clans, web tools and services. Nucleic Acids Res. 2006;34: D247–51.
[36] Bonen L. *Cis*- and *trans*-splicing of group II introns in plant mitochondria. Mitochondrion 2008;8:26–34.
[37] Maxwell DP, Wang Y, McIntosh L. The alternative oxidase lowers mitochondrial reactive oxygen production in plant cells. Proc. Natl. Acad. Sci. U. S. A. 1999;96:8271–6.
[38] Nelson O, Pan D. Starch synthesis in maize endosperms. Annu. Rev. Plant Physiol. Plant Mol. Biol. 1995;46:475–96.
[39] Satoh H, Omura T. New endosperm mutations induced by chemical mutagens in rice *Oryza sativa* L.. Japan J. Breed 1981;3:316–26.
[40] Long W, Dong B, Wang Y, Pan P, Wang Y, Liu L, Chen X, Liu Xi, Liu S, Tian Y, Chen L, Wan J. *FLOURY ENDOSPERM8*, encoding the UDP-glucose pyrophosphorylase 1, affects the synthesis and structure of starch in rice endosperm. J. Plant Biol. 2017;60:513–22.
[41] Peng C, Wang Y, Liu F, Ren Y, Zhou K, Lv J, Zheng M, Zhao S, Zhang L, Wang C, Jiang L, Zhang X, Guo X, Bao Y, Wan J. *FLOURY ENDOSPERM6* encodes a CBM48 domain-containing protein involved in compound granule formation and starch synthesis in rice endosperm. Plant J. 2014;77:917–30.
[42] Wei X, Jiao G, Lin H, Sheng Z, Shao G, Xie L, Tang S, Xu Q, Hu P. *GRAIN INCOMPLETE FILLING 2* regulates grain filling and

starch synthesis during rice caryopsis development. J. Integr. Plant Biol. 2017;59:134–53.
[43] Kubo A, Fujita N, Harada K, Matsuda T, Satoh H, Nakamura Y. The starch-debranching enzymes isoamylase and pullulanase are both involved in amylopectin biosynthesis in rice endosperm. Plant Physiol. 1999;121:399–410.
[44] Matsushima R, Maekawa M, Fujita N, Sakamoto W. A rapid, direct observation method to isolate mutants with defects in starch grain morphology in rice. Plant Cell Physiol. 2010;51:728–41.
[45] Matsushima R, Maekawa M, Kusano M, Kondo H, Fujita N, Kawagoe Y, Sakamoto W. Amyloplast-localized SUBSTANDARD STARCH GRAIN4 protein influences the size of starch grains in rice endosperm. Plant Physiol. 2014;164:623–36.
[46] Matsushima R, Maekawa M, Kusano M, Tomita K, Kondo H, Nishimura H, Crofts N, Fujita N, Sakamoto W. Amyloplast membrane protein SUBSTANDARD STARCH GRAIN6 controls starch grain size in rice endosperm. Plant Physiol. 2016;170:1445–59.
[47] Cosségal M, Vernoud V, Depège N, Rogowsky P. The embryo surrounding region. Plant Cell Monographs 2007;8:57–71.
[48] Ishimaru T, Ida M, Hirose S, Shimamura S, Masumura T, Nishizawa NK, Nakazono M, Kondo M. Laser microdissection-based gene expression analysis in the aleurone layer and starchy endosperm of developing rice caryopses in the early storage phase. Rice 2015;8:57.
[49] Keren I, Tal L, des CC, Francs-Small, Araujo WL, Shevtsov S, Shaya F, Fernie AR, Small I, Ostersetzer-Biran O. nMAT1, a nuclear-encoded maturase involved in the *trans*-splicing of *nad1* intron 1, is essential for mitochondrial complex I assembly and function. Plant J. 2012;71:413–26.
[50] Wang CD, Aube F, Planchard N, Quadrado M, Dargel-Graffin E, Nogue F, Mireau H. The pentatricopeptide repeat protein MTSF2 stabilizes a *nad1* precursor transcript and defines the 3′ end of its 5′-half intron. Nucleic Acids Res. 2017;45: 6119–34.
[51] Haili N, Arnal N, Quadrado M, Amiar S, Tcherkez G, Dahan J, Briozzo P, des Francs-Small CC, Vrielynck N, Mireau H. The pentatricopeptide repeat MTSF1 protein stabilizes the nad4 mRNA in Arabidopsis mitochondria. Nucleic Acids Res. 2013;41:6650–63.
[52] Zhang YF, Suzuki M, Sun F, Tan BC. The mitochondrion-targeted PENTATRICOPEPTIDE REPEAT78 protein is required for *nad5* mature mRNA stability and seed development in maize. Mol. Plant 2017;10:1321–33.
[53] Ren RC, Wang LL, Zhang L, Zhao YJ, Wu JW, Wei YM, Zhang XS, Zhao XY. DEK43 is a P-type pentatricopeptide repeat protein responsible for the *Cis*-splicing of *nad4* in maize mitochondria. J. Integr. Plant Biol. 2020;62:299–313.
[54] Wu MW, Zhao H, Zhang JD, Guo L, Liu CM. *RADICLELESS 1 (RL1)*-mediated *nad4* intron 1 splicing is crucial for embryo and endosperm development in rice (*Oryza sativa* L.). Biochem. Biophys. Res. Commun. 2020;523:220–5.
[55] Zhu C, Jin G, Fang P, Zhang Y, Feng X, Tang Y, Qi W, Song R. Maize pentatricopeptide repeat protein DEK41 affects *cis*-splicing of mitochondrial *nad4* intron 3 and is required for normal seed development. J. Exp. Bot. 2019;70:3795–808.
[56] Murayama M, Hayashi S, Nishimura N, Ishide M, Kobayashi K, Yagi Y, Asami T, Nakamura T, Shinozaki K, Hirayama T. Isolation of Arabidopsis *ahg11*, a weak ABA hypersensitive mutant defective in *nad4* RNA editing. J. Exp. Bot. 2012;63:5301–10.
[57] Hölzle A, Jonietz C, Torjek O, Altmann T, Binder S, Forner J. A RESTORER OF FERTILITY-like PPR gene is required for 5′-end processing of the *nad4* mRNA in mitochondria of *Arabidopsis thaliana*. Plant J. 2011;65:737–44.